OXFORD GENETICS

Preventing evolutionary rescue in cancer using two-strike therapy

Srishti Patil[1,2,3], Armaan Ahmed[4,5], Yannick Viossat[6] and Robert Noble[1,*]

[1]Department of Mathematics, City St George's, University of London, London EC1V 0HB, UK
[2]Indian Institute of Science Education and Research, Pune 411008, India
[3]Division of Theoretical Systems Biology, German Cancer Research Center (DKFZ), 69120 Heidelberg, Germany
[4]Department of Applied Mathematics & Statistics, Johns Hopkins University, Baltimore, MD 21218, USA
[5]Department of Mathematics, Johns Hopkins University, Baltimore, MD 21218, USA
[6]CEREMADE, Université Paris-Dauphine, Université PSL, CNRS, 75016 Paris, France

*robert.noble@city.ac.uk

Abstract

First-line cancer treatment frequently fails due to initially rare therapeutic resistance. An important clinical question is then how to schedule subsequent treatments to maximize the probability of tumour eradication. Here, we provide a theoretical solution to this problem by using mathematical analysis and extensive stochastic simulations within the framework of evolutionary rescue theory to determine how best to exploit the vulnerability of small tumours to stochastic extinction. Whereas standard clinical practice is to wait for evidence of relapse, we confirm a recent hypothesis that the optimal time to switch to a second treatment is when the tumour is close to its minimum size before relapse, when it is likely undetectable. This optimum can lie slightly before or slightly after the nadir, depending on tumour parameters. Given that this exact time point may be difficult to determine in practice, we study windows of high extinction probability that lie around the optimal switching point, showing that switching after the relapse has begun is typically better than switching too early. We further reveal how treatment efficacy and tumour demographic and evolutionary parameters influence the predicted clinical outcome, and we determine how best to schedule drugs of unequal efficacy. Our work establishes a foundation for further experimental and clinical investigation of this evolutionarily-informed multi-strike treatment strategy.

Keywords: mathematical oncology; evolutionary therapy; evolutionary rescue; therapeutic resistance; cancer treatment; extinction therapy

Introduction

Just as species in an ecosystem interact, compete for resources, adapt to changing environmental conditions and undergo natural selection, so cancer clones rise and fall in a tumour ecosystem. Darwinian principles inevitably determine therapeutic responses (Iwasa *et al.* 2006) including the emergence of resistance, which, despite pharmaceutical advances, remains the greatest challenge in oncology. As cancer cells can use a variety of adaptive strategies to achieve resistance (Pressley *et al.* 2021), targeting a single molecular mechanism often proves ineffective in the long term (Greaves and Maley 2012). Understanding intratumour evolutionary processes provides a rational foundation for developing treatment strategies that, by explicitly accounting for evolutionary dynamics, achieve better clinical outcomes (Korolev *et al.* 2014; Enriquez-Navas *et al.* 2015; Aktipis *et al.* 2011). Mathematical modelling of clonal dynamics and the emergence of resistance is critical for optimising clinical treatment strategies based on evolutionary principles. Consequently, the historical development of evolutionary therapies has followed a trajectory that begins with a theoretical and mathematical exploration of associated eco-evolutionary models (West *et al.* 2023).

The clinical strategy we study here uses evolutionary rescue theory to inform the probability of tumour extinction under multiple treatment administrations or "strikes". Although the term evolutionary rescue arose in a conservation context (Gomulkiewicz and Holt 1995), the same theory is applicable when extinction is the goal, such as in bacterial infections or cancer (Coldman and Goldie 1983; Alexander *et al.* 2014; Torres-Barceló *et al.* 2014). Since an oncologist can influence the tumour environment, they can anticipate the evolutionary trajectories of cancer clones and, in theory, follow a strategy to avoid evolutionary rescue and so cure the patient (Gatenby *et al.* 2019). The key idea is that, even if a single strike fails to eradicate cancer cells due to resistant phenotypes, it can still leave the population small and fragmented. The probability that a resistant phenotype in the population leads to evolutionary rescue decreases, rendering the population more vulnerable to stochastic extinction (Torres-Barceló *et al.* 2014). Moreover, a small population is less able to adapt to environmental changes owing to loss of genetic variation (Alexander *et al.* 2014). Cell proliferation may also slow due to Allee effects (Dennis *et al.* 2016) during tumour initiation due to processes like angiogenesis and growth factor signalling (Sewalt *et al.* 2016; Gerlee *et al.* 2022; Azimzade *et al.* 2021). Subsequent therapeutic strikes, if well timed, might be able to exploit these weaknesses to drive the cancer cell population to extinction (Gatenby and Brown 2020).

The main differences between conventional cancer treatment strategies and multi-strike therapy are in the timing of the strikes and the use of evolutionary principles to guide clinical decision making. In combination therapy, multiple drugs with collateral sensitivities are administered simultaneously (Chakrabarti and Michor 2017). In conventional sequential therapy, a second

treatment is typically started during relapse, when the first treatment has evidently failed. In multi-strike therapy (also known as extinction therapy (Gatenby and Brown 2020)), the idea is instead to switch treatments when the tumour is at its weakest, when it may well be clinically undetectable. The success rate of multi-strike therapy is expected to be highly sensitive to the timing and severity of the second and any subsequent strikes. Based on computational modelling, Gatenby *et al.* (2020) have suggested that the best time to switch to the second treatment occurs while the tumour is still shrinking in response to the first treatment.

Demonstrating its potential to improve cure rates across diverse cancer types, multi-strike therapy is being investigated in three small clinical trials. A Phase 2 trial using conventional chemotherapy drugs in metastatic rhabdomyosarcoma started recruiting patients in 2020 and is expected to run until 2026 (NCT04388839). A Phase 1 trial in metastatic prostate cancer (2022-27) involves agents that exploit the hormone sensitivity of cancer cells (NCT05189457). A Phase 2 trial using targeted therapies in metastatic breast cancer began in 2024 (NCT06409390). Further trials are in development.

Yet, despite this rapid progress to clinical evaluation, many critical questions regarding the timing of the subsequent strikes, the time until extinction, the effect of environmental and demographic factors, and most importantly, the conditions under which multi-strike therapy is a feasible alternative to other therapies remain unanswered. What is the probability that a population is rescued either by pre-existing mutants or those that arise during the treatment? How can we maximise the probability of the tumour being eliminated with the second strike? How do outcomes vary with the cost of resistance, density dependence, and other factors that affect clonal growth rates?

We tackle these pressing questions in two ways. First, using ideas from evolutionary rescue theory, we develop and study the first analytical model of two-strike therapy. This simple, tractable mathematical model enables us to compute extinction probabilities and to identify the optimal time for the second strike. Second, we use extensive stochastic simulations to test the robustness of our analytical results and to study the effects of additional factors. Our model only focuses on cases where single-strike therapy and other conventional therapies result in tumour relapse with high probability. The aim is to investigate the feasibility of two-strike therapy when we know that conventional treatments fail to be curative. We thus establish a necessary foundation for further theoretical, experimental, and clinical investigations of multi-strike therapy.

Methods

To obtain general, robust insights into the factors that determine a successful two-strike treatment strategy, we combine an analytical model and a stochastic simulation model. Both models involve two stressful environments (corresponding to the two treatment strikes) and four cell types. The first treatment (or strike) creates a stressful environment that we denote E_1. After switching to the second treatment, the tumour enters the second stressful environment, E_2. We do not take into account treatment toxicity. Cells can be sensitive to both treatments (S), completely resistant to one treatment but sensitive to the other (R_1 and R_2), or completely resistant to both treatments ($R_{1,2}$). The time to switch to the second treatment is τ and the population size at this time is $N(\tau)$. Therefore, when the population size reaches the switching threshold $N(\tau)$, the first treatment is stopped and the second treatment begins.

Analytical methods

Our analytical modelling method is composed of two stages (Figure 1(A)). First, we model the population dynamics during the first treatment as a set of numerically-solved ordinary differential equations (ODEs). We then use those solutions to predict extinction probability using evolutionary rescue theory (as reviewed in Appendix 2: Using results from evolutionary rescue theory). We thus use a deterministic model to represent a stochastic phenomenon. The interpretation is that the quantities $S(t)$, $R_1(t)$, $R_2(t)$ and $R_{1,2}(t)$ in the ODE model are the expected numbers of S, R_1, R_2 and $R_{1,2}$ cells at time t, respectively. In Appendix 4: Correspondence between the analytic evolutionary rescue model and the linear birth-death-mutation model, we verify that the dynamics of the ODE system and the mean dynamics of the corresponding stochastic process are in close agreement. Given this, we verify that the two approaches generate similar numbers of rescue mutants and similar extinction probabilities.

We use the following vocabulary. A potential rescue lineage is a lineage of cells with positive fitness at all future times. In our model these lineages comprise all $R_{1,2}$ cells (since they have a positive fitness in both E_1 and E_2), R_2 cells present at the switching time, and R_2 cells that arise after the switch. While R_1 cells have a positive fitness during treatment 1, they are counterselected during treatment 2 and so cannot rescue the population. Founders of potential rescue lineages are called potential rescue mutants. Potential rescue lineages that escape stochastic extinction and cause evolutionary rescue are called rescue lineages, and their founders are rescue mutants. Rescue mutants already present at the switching time τ are called *pre-existing* rescue mutants, or *standing genetic variants*. Those appearing after are called *de-novo* rescue mutants.

To calculate the extinction probability of the population, we consider the expected number of rescue mutants generated throughout the course of treatment. We must therefore obtain the population composition at the beginning of the second strike. We use the system of differential equations given in Figure 1(A), describing logistic growth in environment E_1 of the four subpopulations $S(t)$, $R_1(t)$, $R_2(t)$ and $R_{1,2}(t)$ that make up the tumour cell population $N(t)$. The model includes mutations from less resistant to more resistant states while, for simplicity, omitting negligible back mutations.

For plausible parameter values, a tumour that grows from a single treatment-sensitive (S) cell is unlikely to harbour any doubly-resistant ($R_{1,2}$) cells at the time it is first treated (see Appendix 1: Analytic Model Without Competition for a reference case for initial resistant populations). If this were not so then extinction would be highly improbable. We therefore assume $R_{1,2}(0) = 0$. Other default initial conditions and parameter values are listed in Table 1. By solving the differential equations numerically over the course of the first treatment (time 0 to time τ), we determine the expected subpopulation sizes at the time of switching to the second treatment.

Given the population dynamics using treatment switching time τ, we next compute the probabilities $P_E^{\mathrm{SGV}}(\tau)$ and $P_E^{\mathrm{DN}}(\tau)$. These are the probabilities of no evolutionary rescue due to standing genetic variation before the beginning of the second treatment and *de-novo* mutations during the second treatment, respectively (Part 2 in Figure 1(A)). Since successful treatment requires the eradication of both pre-existing and *de-novo* mutants during the second treatment period E_2, the tumour extinction

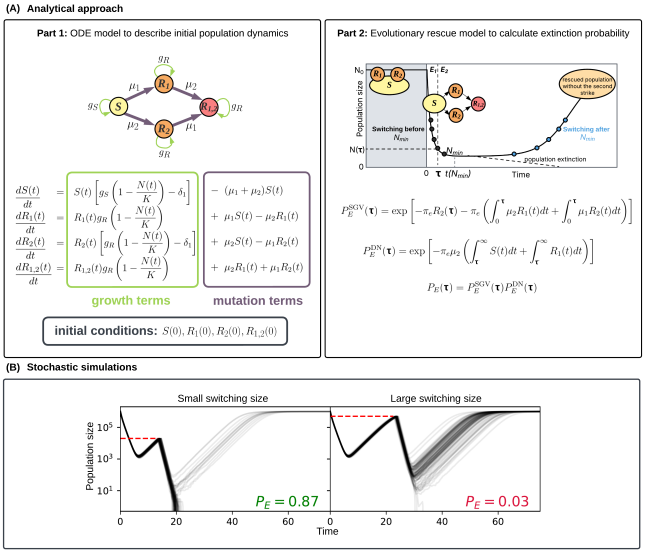

Figure 1 Description of the analytical approach and stochastic simulations. (A): Part 1 (left) shows the ODE population growth model during the first treatment (in E_1). Part 2 (right) uses evolutionary rescue theory and output from the ODE model to calculate extinction probability after the second strike (in E_2). Sensitive cells are denoted by S. Cells resistant to treatment 1(2) and sensitive to treatment 2(1) are denoted by $R_1(R_2)$. Cells resistant to both treatments are denoted by $R_{1,2}$. The per capita rate of acquiring resistance to treatment 1(2) is denoted by $\mu_1(\mu_2)$. Growth rates g_S for sensitive cells and g_R for resistant cells depend on the intrinsic birth rate, intrinsic death rate and the cost of resistance (see Table 1). The treatment-induced death rate, or treatment efficacy in $E_1(E_2)$ is denoted by $\delta_1(\delta_2)$. Initial conditions are specified by the initial population sizes of S, R_1, R_2 and $R_{1,2}$ cells (before the beginning of the first treatment). The total initial population $N(0)$ is the sum of these four subpopulations. As shown in Part 2, the switch to the second treatment can occur before (black dots) or after (blue dots) the population nadir ($N_{\min}$). The solid curve shows the population trajectory with treatment 1 only and the black dashed line shows a possible trajectory to extinction after the switch to the second treatment at time τ. Equations to calculate extinction probability (P_E) are shown. **(B):** Results of two sets of stochastic simulations are shown, illustrating the difference in extinction probabilities due to two different switching sizes (red dashed lines). Extinction probabilities from the simulations are estimated for each switching size as the proportion of extinction outcomes in 100 independent runs. Grey lines show individual simulation runs. The stochastic simulation model is independent of the analytical approach, and is described in Methods.

probability $P_E(\tau)$ is the product of these two probabilities:

$$\begin{aligned} P_E(\tau) &= P_E^{\mathrm{SGV}}(\tau) P_E^{\mathrm{DN}}(\tau) \\ &= \exp\left[-\pi_e\left(R_2(\tau) - \int_0^\tau \mu_2 R_1(t) + \mu_1 R_2(t) dt \right.\right. \\ &\quad \left.\left. -\mu_2 \int_\tau^\infty S(t) + R_1(t) dt\right)\right], \end{aligned} \tag{1}$$

where π_e is the probability of establishment of a single potential rescue lineage, that is, of a mutant lineage with positive fitness. This probability depends on the birth rate (b), death rate (d) and cost of resistance (c). See Appendix 5: Derivation of the establishment probability and Appendix 3: Derivation of extinction probabilities for more details on the derivation of Eq 1. A key assumption is that the number of rescue mutants is Poisson distributed, which introduces the negative exponential in the expression. Equation 1 also assumes that the probability of extinction during E_1 in the expression for total extinction probability is negligible. We verify this assumption at the end of Appendix 1: Analytic Model Without Competition, where we compare extinction probabilities from single-strike and two-strike therapies. This holds for all our parameter values.

With Eq 1, we study the behaviour of extinction probability as a function of τ under different conditions. The absolute value of the quantity in the exponent represents the total expected number of rescue mutants generated if we switch at time τ. The first term represents the expected number of R_2 cells present at the switching time, multiplied by the probability that they get established. The next term $(\pi_e \int_0^\tau \mu_2 R_1(t) + \mu_1 R_2(t)\, dt)$ represents the total expected number of established $R_{1,2}$ mutants generated by mutation from either R_1 or R_2 cells during E_1. The last term $(\pi_e \mu_2 \int_0^\tau S(t) + R_1(t)\, dt)$ computes the expected number of established R_2 and $R_{1,2}$ cells generated by mutation from S and R_1 cells during E_2. The dynamics of the population during E_2 are modelled using the system of differential equations given in Eqs 28-29. There is no explicit $R_{1,2}$ term because we assume $R_{1,2}(0) = 0$, and only the number of $R_{1,2}$ lineages (not the number of cells) generated throughout the entire treatment is required to calculate the extinction probability. Note that we do not compute the number of rescue mutants in the same way for $R_{1,2}$ cells and R_2 cells. As R_2 cells have a positive fitness only in environment E_2, we consider as potential founders of rescue lineages the R_2 cells that are present when switching to treatment 2 and those that arise later by mutation of S cells. By contrast, $R_{1,2}$ cells have positive fitness and the same establishment probability in both environments E_1 and E_2. Thus, the expected number of $R_{1,2}$ rescue mutants is simply this establishment probability multiplied by the expected number of $R_{1,2}$ lineages, which is the expected number of $R_{1,2}$ cells present at time 0 or arising by mutation, whether in E_1 or E_2.

In Appendix 1: Analytic Model Without Competition, we describe a model for two-strike therapy without competition. By removing the carrying capacity from the ODE model in Figure 1(A) we obtain a system of linear differential equations which has an explicit solution (Eqs 8-10). Using this solution, we derive expressions for the expected number of rescue mutants (Eq 13) and the population nadir. Since extinction probability is maximised when the expected number of rescue mutants is minimised, we find the optimal switching size and compare it to the nadir. We also compare our main results, which are derived under the assumption of a large initially resistant population, to a reference case corresponding to mutation-selection balance in an exponentially growing population. Further, we use this model to provide

Table 1 List of parameters and initial conditions used in the analytical and stochastic simulation models, along with their default values. Note that for the analytical model, we use the values of growth rates for sensitive and resistant cells, $g_S = b - d$ and $g_R = b - c - d$, respectively. The birth rate (b), death rate (d), cost of resistance (c) and rates of acquiring resistance (μ_1, μ_2) are expressed in per-day units. For more details on parametrisation, see Methods.

Symbol	Description	Default value
K	Carrying capacity of the system	$N(0)$
b	Per capita birth rate of S cells	1.0
d	Per capita death rate of all cell types	0.1
c	Cost of resistance	0.5
μ_1, μ_2	Mutation rate for acquiring resistance to treatment 1, 2	2.5×10^{-6}
δ_1, δ_2	Per capita death rate due to treatment 1,2	2.0
$S(0)$	Initial population of S cells	10^6
$R_1(0)$	Initial population of R_1 cells	100
$R_2(0)$	Initial population of R_2 cells	100
$R_{1,2}(0)$	Initial population of $R_{1,2}$ cells	0

intuition for our results and examine the effects of changing model assumptions, such as removing the cost of resistance.

Stochastic simulations

To test the robustness of our analytical results, we separately obtain extinction probabilities using a stochastic simulation model with the same initial conditions as the ODE system and equivalent default parameter values. The main difference between the models is that the analytical method uses evolutionary rescue theory to calculate extinction probabilities, whereas the computational approach uses the stochastic Gillespie algorithm to simulate birth, death, and mutation events. Density dependence is implemented in the birth rates used for the simulations. Each simulation ends with one of three outcomes: extinction, progression, or persistence (see Table A.2). Progression is when the total population at the end of the simulation is greater than the total initial population. Persistence is when the population does not go extinct but is smaller than the initial population. The extinction probability is estimated for each switching size as the proportion of extinction outcomes in a large number of independent simulations. See Appendix 7: Stochastic Simulation Model for a detailed description of the stochastic simulation model.

Comparing results across parameter values

To compare treatment outcomes for varied parameter values, we use a summary variable N_q to describe how small the tumour must be at the time of switching treatment to achieve a given probability of extinction. This concept is based on our observation that the extinction probability $P_E(\tau)$ generally decreases as $N(\tau)$ increases, unless $N(\tau)$ is very close to the population nadir ($N_{\min}$) that would pertain if we were to continue the first treatment instead of switching to a second treatment. Therefore, for a given extinction probability q (with $0 \leq q \leq \max(P_E(\tau))$), we can obtain a corresponding value N_q, which is the maximum population size threshold below which we achieve an extinction probability greater than or equal to q. In other words, if $N(\tau) \leq N_q$, then we will achieve an extinction probability of at least q. Any given switching size $N(\tau)$ greater than $N_{\min}$ is reached twice in the trajectory of a population undergoing evolutionary rescue during the first treatment, once before and once after the start of relapse (see Figure 1(A), right for an illustration). N_q is therefore defined for both the before-nadir and after-nadir switching sizes:

$$N_q^{(\text{before})} = \max\{N(\tau) : P_E(\tau) \geq q, \tau < t(N_{\min})\},$$
$$N_q^{(\text{after})} = \max\{N(\tau) : P_E(\tau) \geq q, \tau > t(N_{\min})\},$$

where $t(N_{\min})$ is the time at which the nadir would be reached in the absence of a second strike.

N_q values tell us when and how fast the extinction probability drops from a high to a low value. For example, if the difference between $N_{0.1}^{(\text{before})}$ and $N_{0.9}^{(\text{before})}$ is slight, it means that the extinction probability goes from a low value to a high value without much change in the population size. Therefore, the extinction probability increases steeply with N. If $N_{0.1}^{(\text{before})}$ and $N_{0.9}^{(\text{before})}$ are far apart, there is a more gradual increase in extinction probabilities as the population size decreases. The value of q where the N_q curve "cuts off" (as seen in Figure A.1) is the highest extinction probability possible with a given set of parameters. We plot N_q versus q to analyse the trend in extinction probabilities across the range of potential switching sizes and parameter values.

When comparing different parameter values, a higher N_q curve indicates better treatment outcome. This is because it is favourable to reach high extinction probabilities at large switching sizes. For instance, a higher value of $N_{0.9}$ implies a wider window of opportunity due to a wider range of switching sizes for implementing a successful second strike. Furthermore, if we have two N_q curves corresponding to different sets of parameter values and one curve lies above the other, then in the case corresponding to the higher curve we can achieve a higher extinction probability for a given switching size (as illustrated in Figure A.1). The parameter values corresponding to the uppermost N_q curve are therefore expected to result in a better treatment outcome in terms of ease of implementation, higher extinction probabilities, or both.

Parametrisation

The default parameters used for the stochastic simulations and numerical solutions are listed in Table 1. To facilitate comparison with previous research (Gatenby *et al.* 2020), we set the carrying capacity equal to the total initial population size, yet we also show that our results are highly robust to varying the carrying capacity. By default, we assume a large cost of resistance (half of the intrinsic birth rate), but we also study in detail the case in which resistance has no cost. We conservatively set the size of the initial resistant populations (before the first treatment begins) to 10^{-4} times the initial sensitive population, which is larger than the resistant population size predicted using a reasonable growth model (see Appendix 1: Analytic Model Without Competition for a reference case for initial resistant populations). We also consider the case $R_2(0) = 0$.

The intrinsic birth and death rates are of the same order of magnitude as those reported in the literature and used in prior mathematical modelling (Gatenby *et al.* 2020). Since the rate of acquiring resistance (which we will call the mutation rate)

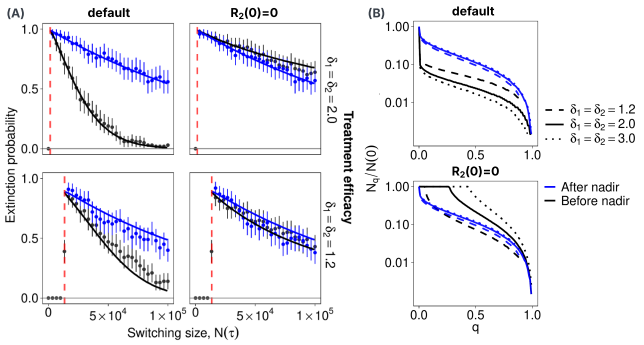

Figure 2 Optimal switching sizes. (A): Extinction probabilities $P_E(\tau)$ obtained from the stochastic simulations (dots) and the analytical approach (solid line) for different switching sizes $N(\tau)$, implemented before reaching the nadir $N_{\min}$ (black) and after crossing $N_{\min}$ (blue). Red dashed lines show the expected $N_{\min}$ (calculated with the analytical model). Results for two treatment efficacies are shown (rows). Columns show results for the default parameter set (Table 1) and for the case when $R_2(0) = 0$. Extinction probabilities from the simulations are estimated for each switching size as the proportion of extinction outcomes in 100 independent runs. In almost all simulations, switching sizes smaller than $N_{\min}$ prove unattainable, so the switch never occurs and the extinction probability is close to zero (black points to the left of red dashed lines). Error bars show 95% binomial proportion confidence intervals. **(B):** Normalised N_q vs q plots (described in Methods) for the default parameter set and for $R_2(0) = 0$ with different treatment efficacies (δ_1=δ_2). Black curves show before-nadir switching sizes, and blue curves show after-nadir switching sizes.

varies depending on cancer type, treatment types, and patient attributes, we focus on a mutation rate corresponding to clinical scenarios in which two-strike therapy is worth considering. Much higher mutation rates render two-strike therapy ineffective, whereas lower mutation rates result in higher extinction probabilities (Figure A.7).

Results

To enable us to uncover general principles and determine the most important factors in a successful treatment strategy, we consider the simplest case of two strikes. Since further strikes can only increase extinction probabilities, we thus obtain conservative lower bounds on potential clinical benefits. We obtain extinction probabilities using both an analytical evolutionary rescue model and a stochastic simulation model (see Methods), and we compare the two wherever possible. Unless stated otherwise, we use a default set of parameters and initial conditions (Table 1), and assume the two treatments induce identical death rates (that is, δ_1=δ_2=δ). For brevity, we will use "treatment efficacy" to refer to these treatment-induced death rates, which in reality also depend on pharmacodynamics and pharmacokinetics.

Our focus will be on the population size at the time of switching between the two treatments, denoted $N(\tau)$. Since the optimal $N(\tau)$ (the value corresponding to the highest extinction probability) changes as we vary parameter values, the trend of extinction probabilities obtained at a fixed $N(\tau)$ could differ from the trend obtained at the optimal $N(\tau)$. The rationale for using a fixed $N(\tau)$ for such comparisons is that it may in practice be impossible to determine the optimum. The fixed $N(\tau)$ can be implemented on either side of the population nadir reached in the absence of a second strike ($N_{\min}$). The population nadir can be calculated by numerically solving the system of differential equations shown in Figure 1(A) (see Appendix 1: Analytic Model Without Competition for an analytical approximation). We consider both before-nadir and after-nadir switching sizes (Figure 1(A), right).

Throughout this section, we use two key metrics to compare different parameter values and treatment conditions. The first is the range of high-P_E switching sizes, defined as the difference in the largest and smallest switching sizes that result in an extinction probability of at least 0.8. The second metric compares N_q curves with the rule of thumb that a higher-lying curve indicates a better treatment outcome (see Figure A.1). As defined in Methods, N_q is the maximum switching size to achieve an extinction probability greater than or equal to q.

The optimal switching size is close to the population nadir

Our first aim is to find the optimal population size, $N(\tau)$, at which to switch from the first to the second treatment. Our analytical and stochastic models both show that the optimal $N(\tau)$, in terms of maximizing extinction probability, is close to the population nadir $N_{\min}$ (Figure 2). According to the analytical model, the optimal switching size may, depending on parameter values, lie slightly before or after $N_{\min}$ (Appendix 1: Analytic Model Without Competition). Yet the difference between the optimal $N(\tau)$ and the $N_{\min}$ is generally so small that it is not captured by our simulation results. The difference is significant only when R_2 cells are initially abundant and the cost of resistance is low (Figure A.2, second column).

To explain why the optimal $N(\tau)$ is close to $N_{\min}$, we refer to Eq 1 and see that the maximum $P_E(\tau)$ will be achieved by minimizing the sum of all the rates of generating rescue mutants. Note that even though the sum of S and R_1 is minimized at $N_{\min}$, the *de-novo* rescue terms (the last two integral terms in Eq 1) are minimized slightly after $N_{\min}$. This is because the increase in the number of cells after $N_{\min}$ is balanced by the faster decay of R_1 cells due to their cost of resistance. It follows that the *de-novo* rescue probability will be minimized when we have more R_1 cells and fewer S cells, even if the total number of cells is higher.

To minimize the rescue probability due to pre-existing mutants at the start of the second strike (the first three terms in Eq 1), we focus on the decay of the R_2 population and the emergence of $R_{1,2}$ mutants. Their relative rates determine where the switching size minimizing the number of pre-existing rescue mutants falls in relation to $N_{\min}$. For further analysis, we focus on regions of high extinction probability ($P_E \geq 0.8$) instead of the exact optima. Consistent with our analytical predictions, we observe that these high-P_E regions lie around $N_{\min}$ (Figures 2 and A.2).

It is better to implement the second strike after the nadir than before

Given the practical impossibility of treating at the exact optimal time, we next compare outcomes for treating earlier or later. While the optimal switching size may lie slightly before or after the nadir, we observe that switching sizes implemented after $N_{\min}$ usually have higher extinction probabilities than those before $N_{\min}$ (Figure 2(A), left column and (B), top panel).

We hypothesize that this result is due to the pre-existing (or initially accumulated) R_2 population. If we delay switching, then this resistant subpopulation has longer to decay, which results in a smaller rescue population during the second treatment. On the other hand, there is more time for doubly-resistant $R_{1,2}$ mutants to accumulate. In most cases of interest, the generation of $R_{1,2}$ mutants is slower than the decay of the R_2 population, and so the window of opportunity for effective treatment extends further to the right of the nadir than to the left. In Appendix 1: Analytic Model Without Competition, we derive this result for the analytical model without competition.

Assuming that R_2 cells are absent at the start of the first treatment substantially increases extinction probabilities for before-nadir switching (Figure 2(A), right column and (B), bottom panel; Figure A.2). The result of switching before the nadir is then similar to – or, in the case of a high-efficacy treatment, even slightly better than – the result of switching at the same tumour size after the nadir.

Higher efficacy of the first treatment is not necessarily beneficial for treatment

Since treatment toxicity is a major concern in cancer therapy, we now relax our assumption that the two treatments have equal efficacy, enabling us to investigate the potential for using lower, more tolerable doses. For alternative combinations of δ_1 (efficacy of the first treatment) and δ_2 (second treatment), we consider both the optimal switching size and the range of $N(\tau)$ values that lead to a high extinction probability ($P_E \geq 0.8$). We will refer to treatment efficacies of 2 and 1.2 (relative to the default intrinsic birth rate of sensitive cells) as high and low, respectively.

We first consider the before-nadir regime. The intuitive prediction is that a higher treatment efficacy should lead to a larger range of high-P_E switching sizes. This is what we observe in the case of no resistance cost and $R_2(0) = 0$ (Figure 3(A), right). However, for our default parameter values, higher values of δ_1 give smaller ranges of high-P_E switching sizes (Figure 3(A), left). Similarly, in the before-nadir regime, lower treatment efficacies result in higher extinction probabilities for all switching sizes that are not very close to $N_{\min}$ (Figure 3(B,C) and 2(B), top). A normalised N_q versus q plot for four δ_1-δ_2 combinations confirms that low δ_1 plus high δ_2 produces the best treatment outcome in terms of the range of high-P_E switching sizes, because it gives a higher extinction probability at the same $N(\tau)$ (Figure 3(C)). When the two treatments are equally effective, we observe a similar trend (see Figure 2(B), top panel and Figure A.8(C)). Thus, for our default parameter values, a low-efficacy first treatment paired with a high-efficacy second treatment gives the largest window of opportunity when switching before the nadir.

The somewhat counter-intuitive result is explained by the interaction of the treatment efficacy, the cost of resistance, and the R_2 population. For lower δ_1, the S cells decay more slowly, so the switching size $N(\tau)$ is reached later. This provides more time for the R_2 population to decay, but also more time for $R_{1,2}$ mutants to arise. When the cost of resistance and the initial R_2 population (before the first treatment begins) are both large, the benefit of a lower δ_1 outweighs the disadvantages (see Appendix 1: Analytic Model Without Competition for a formal explanation). Therefore, we do not observe this effect when the cost of resistance or the initial R_2 population size is set to zero (Figure A.6, Figure 3(A), right). Note that if the first treatment's efficacy is too low then the population size will never become small enough to have a non-negligible probability of stochastic

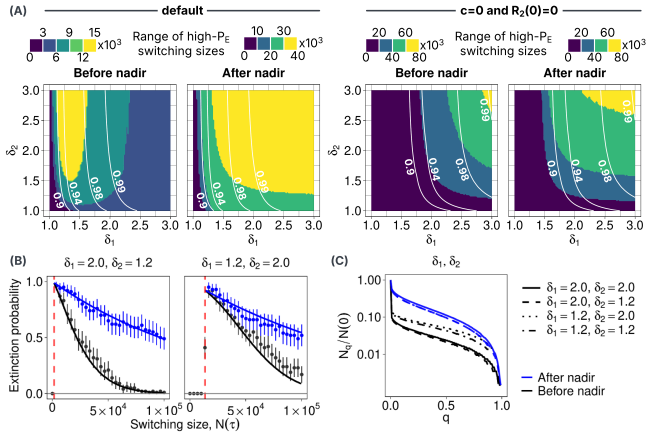

Figure 3 Optimal treatment combinations (A): Heatmaps of the range of high-P_E switching sizes ($P_E \geq 0.8$, obtained from the analytical model) for different combinations of treatment efficacies δ_1 and δ_2. The default case is shown on the left, and the case with no cost of resistance and no initial R_2 population is on the right. For each case, both before-nadir and after-nadir switching sizes are considered. White lines indicate optimal extinction probability contours (highest extinction probability across all switching sizes). Note that the colour scales cover different ranges. **(B):** Extinction probabilities for two combinations of treatment efficacies where $\delta_1 \neq \delta_2$. Dots show simulation results and solid lines indicate analytical model predictions. Red dashed lines show the expected $N_{\min}$ (calculated with the analytical model). Before(after) nadir switching sizes are shown in black(blue). Extinction probabilities from the simulations are estimated for each switching size as the proportion of extinction outcomes in 100 independent runs. Error bars show 95% binomial proportion confidence intervals. **(C):** Normalised N_q vs q plots (see Methods) for four different treatment combinations. Black(blue) lines show before(after)-nadir switching sizes.

extinction.

Although a low δ_1 gives a larger range of high-P_E switching sizes, the highest extinction probability in all cases is obtained when both treatment efficacies are high (white contours in Figure 3(A)). Therefore, it is important to define what we need for a good treatment outcome. The best treatment combination should not only lead to a high extinction probability at the optimal switching size, but it should also offer a large window of opportunity, that is, it should allow a large range of high-P_E switching sizes. A low δ_1 allows a larger window of opportunity than a high δ_1 at the cost of compromising on the optimal extinction probability (0.94 compared to 0.99). Moreover, with a low δ_1, the absolute values high-P_E switching sizes are also high, because the $N_{\min}$ and the range of high-P_E switching sizes are relatively large. We observe this in the right panel of Figure 3(B).

Note that this result depends on the fact that we compare ranges of high-P_E sizes. The conclusion would be different if we were thinking in terms of switching times. A larger value of δ_1 is expected to lead to a larger high-P_E time interval. Thus, the best treatment efficacy in the before-nadir regime depends on how the therapy is implemented.

Outcomes for the after-nadir regime are best when both treatment efficacies are high, at least when thinking in terms of

switching sizes (Figure 3(A), second panel; in terms of switching times, see Figure A.5). For our default parameter values, as expected, the range of high-P_E switching sizes is also much larger for the after-nadir regime than for the before-nadir regime. When we eliminate the cost of resistance and the initial R_2 population, the optimal treatment combinations in the before-nadir and after-nadir regimes are similar (Figure 3(A), fourth panel).

The cost of resistance is not necessarily beneficial for treatment

A cost of resistance is expected to hasten the decay of R_2 mutations during the first treatment phase and so make the second treatment more effective. Accordingly, in most cases, removing the cost of resistance reduces extinction probabilities (see Figure A.2 and A.7(F)). However, in the case of high-efficacy treatment ($\delta = 2$), extinction probabilities for switching sizes implemented well after the nadir can be slightly higher in the absence than in the presence of a resistance cost (but the optimal extinction probability is high even for severe resistance costs). This can be observed in the first panel of Figure 4(A) and (B). The reason for this counter-intuitive result is that in the absence of a cost of resistance and when switching after the nadir, fewer $R_{1,2}$ mutants are generated in the first treatment phase (see the section on the cost of resistance in Appendix 1: Analytic Model Without Competition for a more detailed explanation). If we fix the switching time instead of the switching size, we see that a higher resistance cost is always beneficial for treatment (see Figure 4(C)).

For low-efficacy treatment ($\delta = 1.2$), the main effect of removing the cost of resistance is to increase $N_{\min}$, which makes it impossible to achieve high rates of extinction (Figure 4(A), second panel). We note here that although our analytical predictions are generally very close to our simulation results, they underestimate the probability of extinction when treatment efficacy is low and there is no cost of resistance. In this case, our modelling assumption of a Poisson-distributed R_2 population breaks down. This breakdown occurs when the variance of the R_2 population is higher than that of the corresponding Poisson distribution, which leads to a higher probability that there are no pre-existing rescue mutants when the second treatment commences. Since turnover is a measure of demographic stochasticity, larger values of intrinsic turnover ($b + d$) at a constant intrinsic growth rate ($b - d$) lead to larger variance in the R_2 population and the breakdown of the Poisson assumption (see Appendix 4: Correspondence between the analytic evolutionary rescue model and the linear birth-death-mutation model and Figure A.11 for more details).

Two-strike therapy is feasible only in small tumours

Using the analytical model, we compare different values of N_q (not normalised) for different initial population sizes $N(0)$, bearing in mind that the resistant population size scales with $N(0)$. We observe that the absolute values of N_q for q close to 1 do not vary by more than an order of magnitude when $N(0)$ ranges over three orders of magnitude, from 10^4 to 10^7 cells (Figure 5(A)). This implies that, within this range of initial tumour sizes, a high extinction probability can be achieved by applying the second strike at a sufficiently small population size (determined by the treatment efficacy, growth rates, and other parameters). Nevertheless, if $N(0)$ is larger than 10^8 cells then the extinction probability never exceeds 0.4 (Figure 5(A), dotted lines).

To achieve a 95% extinction probability after switching at the

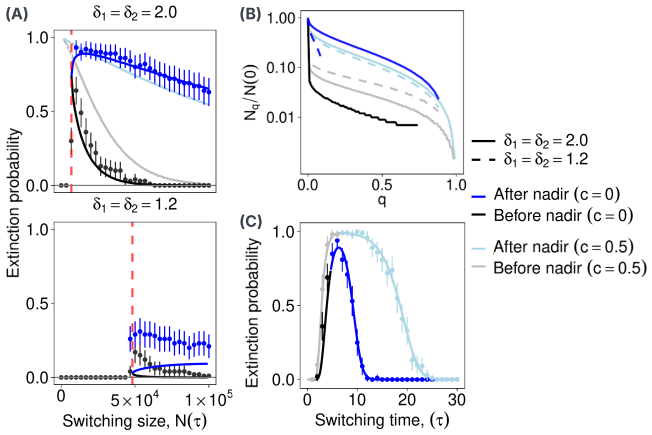

Figure 4 The effect of the cost of resistance. (A): Extinction probabilities without a cost of resistance, for high (top) and low (bottom) treatment efficacies. Dots show simulation results and solid lines indicate analytical model predictions. Before(after) nadir switching sizes are shown in black(blue). Faded lines show the analytical estimates of extinction probabilities in the default case ($c = 0.5$) for reference. Red dashed lines show the expected $N_{\min}$ (calculated with the analytical model). Extinction probabilities from the simulations are estimated for each switching size as the proportion of extinction outcomes in 100 independent runs. Error bars show 95% binomial proportion confidence intervals. **(B):** Normalised N_q vs q plots for two treatment efficacies and zero cost of resistance. Faded lines show the default case ($c = 0.5$) for reference. The before-nadir curve for $c = 0$ and $\delta = 1.2$ overlaps with the $\delta = 2.0$ curve, and ends at $q = 0.05$. **(C):** Time windows of high extinction probability. Solid lines are obtained from Equation 1 under deterministic population dynamics with switching to the second drug at time τ. The dots with 95% confidence intervals are from 100-replicate Gillespie runs.

nadir using our default parameters and without competition (in the large K limit), the initial tumour must be no larger than around 7 million cells. To achieve the same extinction probability using single treatment therapy, the initial tumour must be three to four orders of magnitude smaller (see the last section in Appendix 1: Analytic Model Without Competition for an analytic derivation). There is, therefore, a limit on the size of tumours for which two-strike therapy is likely to succeed, but it is orders of magnitudes larger than for single-strike therapy.

Extinction probability is insensitive to carrying capacity

As the carrying capacity is increased from $N(0)$ (default value), we see a slight increase in extinction probability in the before-nadir regime, but this effect saturates around $K = 10N(0)$. This is demonstrated in Figure 5(B) using the analytical model and in Figure A.8(D) with stochastic simulations. Systems with a lower K have an extra constraint on population growth since the initial population is closer to the carrying capacity. In our model, this results in a higher decay rate for S cells at the beginning of the first strike. Therefore, the switching size $N(\tau)$ (before nadir) is reached earlier and the expected R_2 population size is relatively larger when the switch occurs. This effect is not observed if the R_2 population is initially zero (Figure A.7(C)).

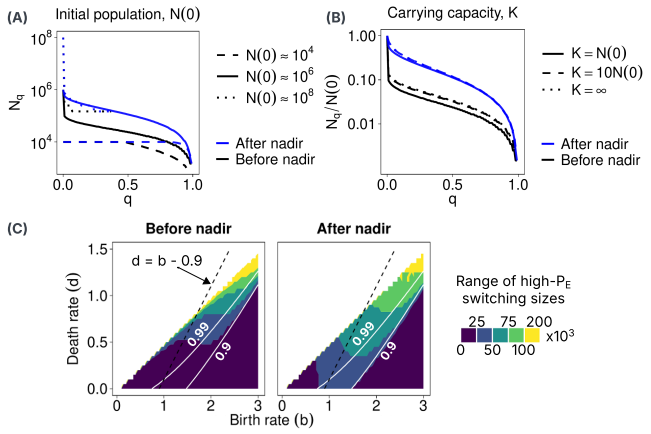

Figure 5 Effects of varying initial population, carrying capacity, birth and death rates. (A): N_q versus q plots for several initial population sizes with the same proportion of initial resistant cells. The x-axes show extinction probability threshold q, and y-axes are the N_q^{before} (black) and N_q^{after} (blue) values. Solid curves correspond to the default parameter values (Table 1). **(B):** Normalised N_q versus q plots for several carrying capacities. The curve for $K = 10N(0)$ overlaps with the curve for $K = \infty$ (no competition). **(C):** Heatmap of the range of high-P_E switching sizes for different parameter values in b-d space. Only non-negative growth rates (excluding the effects of treatment) are considered ($d \leq b - c$). The dashed black line indicates the set of birth and death rates corresponding to our default growth rate ($b - d = g_S = 0.9$). Solid white lines show optimal extinction probability contours (highest extinction probability across all switching sizes).

Extinction probability increases with death rate and turnover

To compare treatment outcomes across different plausible combinations of birth and death rates, we plot heatmaps of the range of high-P_E switching sizes in b-d space (Figure 5(C)). In the lower right region (characterized by high birth rates and low death rates), extinction probabilities are very low. This leaves us with a diagonal band in the b-d space where high extinction probabilities become attainable. We define the "good" region as the area to the left of the the contour line corresponding to an optimal extinction probability of 0.9 (solid white line in Figure 5(C)).

Within this "good" region, we make three major observations. First, a higher death rate results in a higher extinction probability (Figure A.7(E)). Second, as the birth rate increases, optimal extinction probability decreases and the optimal $N(\tau)$ increases (Figure 5(C), first panel and Figure A.7(D)). Faster growth rate of R_1 cells and slower decay of S cells due to increase in b leads to a larger N_{min} and therefore a larger optimal $N(\tau)$ (assuming that the optimal switching size is close to the nadir). The range of high-P_E switching sizes within the "good" region is insensitive to changing the birth rate.

Third, we observe that the range of high-P_E switching sizes becomes larger as we increase the turnover (defined as the sum $b + d$) while keeping the intrinsic growth rate g_S constant (dashed line in Figure 5(B)). Note that the cost of resistance is always a fixed fraction (0.5 by default) of the birth rate of S cells. It follows that when increasing turnover while keeping the growth rate g_S constant, the growth rate g_R of resistant cells decreases. This leads to a smaller resistant population, contributing to the increase in extinction probability. Another effect of turnover relates to the establishment probability of potential rescue lineages. As noted in Appendix 5: Derivation of the establishment probability, turnover appears in the expression for estimating the establishment probability π_e. Higher turnover at a constant net growth rate g_S leads to a lower π_e. Turnover also quantifies the influence of genetic drift, and it has been shown that increasing genetic drift reduces the probability of fixation of mutant cell types (Uecker and Hermisson 2011). If it is harder for potential rescue lineages to establish, then there will be fewer rescue lineages, leading to better treatment outcomes.

Discussion

Here we have developed the first analytical model of a two-strike cancer therapy derived from the principles of evolutionary rescue. Our approach yields clearer explanations and more general results than previous computational modelling (Gatenby *et al.* 2020), in that we perform a more systematic analysis of the parameter space and we obtain extensive analytical results. We have also developed a complementary stochastic simulation model, which generally confirms the accuracy of our analytical predictions. To establish general conditions for successful therapy, we have sought to keep our models simple and conservative, for example by excluding Allee effects and assuming a relatively large initial population of resistant cells.

In terms of methodology, our study differs from the bulk of prior evolutionary rescue models that consider either one abrupt change in the environment or a continuous, gradual change (Bell 2017). While previous studies have examined evolutionary rescue when the environment fluctuates between harsh and favourable states (Greenspoon and Mideo 2017; Marrec and Bitbol 2020; Marrec and Bank 2023), we consider a sequence of distinct harsh states, such that the timing of environmental change is a controllable parameter. Most existing models of evolutionary rescue consider a single resistant variant or, in a few cases (Martin *et al.* 2013; Iwasa *et al.* 2004; Uecker and Hermisson 2016; Osmond *et al.* 2020), multiple variants with respect to one selective pressure. We have instead developed the case with three types of resistance to two types of environmental change, in the spirit of the classic chemotherapy model of Coldman and Goldie (1983).

We have used these new mathematical and computational models to investigate the optimal timing of the second strike and how the treatment outcome depends on crucial system parameters, including treatment efficacies and cost of resistance. The combination of analytical and computational analyses arms us with powerful tools to explore two-strike therapy in a wide range of scenarios, with a solid basis in eco-evolutionary theory. Several of our main conclusions are further supported by numerical results obtained using a different computational model, as reported in a preprint that was posted a year after our own study (Dabi *et al.* 2025).

When do we get the highest extinction probabilities? The ability to analytically predict the optimal switching size for a large range of parameter values promises to aid the design of effective treatment schedules. In contrast to Gatenby *et al.* (2020), who suggested that striking before – even long before – N_{min} is better, we have shown that the optimal switching size is either slightly before or slightly after the nadir. Given that it is unreasonable to expect switching to the second strike exactly at the optimal size, we have shown that it is generally better to wait

slightly longer and risk missing the optimal $N(\tau)$ than to apply the second strike too early. However, one should certainly not wait until the tumour becomes detectable again (as is the current practice) because that increases the probability that rescue mutants will emerge.

Why do our results differ from those of Gatenby et al. (2020)?

The model of multi-strike therapy investigated by Gatenby *et al.* (2020) differs from ours in important respects that account for our contrasting conclusions regarding the optimal timing of the second strike. In their model, the cell population is initially sensitive to the first treatment and resistance to this first treatment is a continuous trait, such that the tumour becomes increasingly resistant while the first treatment is applied. All tumours are assumed to be equally sensitive to the second treatment, which is modelled simply as an instantaneous 20% reduction in tumour size. Moreover, the first treatment is continued after the second strike.

In the absence of density-dependent effects, the second treatment in the model of Gatenby *et al.* (2020) effectively shifts the subsequent population size curve downwards by 20%. If this second strike is applied before N_{min} then the tumour size nadir will be 20% less than N_{min}, rendering the tumour more susceptible to stochastic extinction. Applying the second strike when the tumour size is close to N_{min} is somewhat less effective than applying it earlier because in the latter case the tumour size spends more time below N_{min}. Striking after N_{min} is worse still because by then the tumour is both larger and more resistant to the first treatment. Yet even if it is applied at the optimal time, the second strike's impact on extinction probability will be negligible unless N_{min} happens to be very close to the stochastic extinction threshold.

Gatenby *et al.* (2020) instead found the second strike to be highly effective because they assumed that tumour growth is strongly density dependent. First, they assumed that, due to competition for resources, growth is inhibited at sizes close to the initial population size. Applying the second strike very early is therefore suboptimal as it reduces the benefit of this negative density dependence. Second, and much more consequentially, they assumed that an Allee effect inhibits growth at small population sizes, to the extent that the growth rate becomes negative at sizes moderately below N_{min}, even for maximally resistant cells. Combined with the Allee effect, their second strike sufficed to shrink the tumour beyond the threshold at which extinction is not only probable but inescapable.

In summary, whereas the results of Gatenby *et al.* (2020) pertain to a specific scenario in which the first treatment drives the tumour to the brink of inevitable extinction and a small nudge can tip the balance, we have examined a more general case with more conservative assumptions. In our model, which has no Allee effect, the aim is not to push the tumour size below a given threshold but instead to minimize the probability that a rescue lineage will become established.

What are the best treatment combinations? The treatment efficacies during the two strikes (δ_1 and δ_2) are the easiest model parameters to control in practice. The higher the two treatment efficacies, the higher the extinction probability at the optimal switching size (Figure 3). However, switching at the optimal size, which becomes smaller as the treatment efficacy is increased, may be infeasible. In this case, the treatment combination that gives a wide range of switching sizes with a high probability of extinction may be better. Surprisingly, at least with a high cost of resistance, we found that the largest high-P_E (≥ 0.8) region in the before-nadir regime is obtained with an low-efficacy first treatment paired with a high-efficacy second treatment.

This result emphasizes the importance of timing in two-strike therapy – a stronger treatment with a poorly chosen switching time can be worse than a weaker treatment given at the right time. An interesting implication of this result is that the two treatments need not both be very effective. A low treatment-induced cell death rate can give good treatment outcomes if the cost of resistance is high. Moreover, the optimal switching size is also relatively high for a less effective first treatment, which may be beneficial for treatment in practice.

What other tumour parameters determine the success of two-strike therapy? Our systematic exploration of the model parameter space reveals several noteworthy effects on treatment outcomes. First, although a high cost of resistance is predictably beneficial for treatment, we found that two-strike therapy can outperform conventional sequential treatment even when this cost is small or non-existent (Figure 4). Therefore, in common with adaptive therapy (Viossat and Noble 2021), two-strike therapy is not contingent on a cost of resistance. Moreover, we saw a variable response to a change in the cost of resistance depending on treatment efficacy. For high treatment efficacies, we observed comparable extinction probabilities in the presence and absence of the cost of resistance, but for low efficacies, a small cost of resistance gives much worse treatment outcomes than a high cost.

Second, we find that higher intrinsic death rate and turnover are beneficial for treatment, consistent with findings that higher turnover increases extinction probability (Raatz and Traulsen 2023). This has also previously been shown for adaptive therapy (Strobl *et al.* 2020).

Third, we found that for a given initial tumour size, changes in carrying capacities have little effect on treatment outcome (Figure 5(B)) even though a higher carrying capacity allows more tumour growth. This indicates that two-strike therapy could potentially be applied to both primary and metastatic cancers.

Although we have used simple models with minimal assumptions to ensure that our main findings are qualitatively robust, we have not explored all plausible functional forms. For example, in a model in which mutations occur only at the time of cell division, the number of potential rescue mutants (and therefore extinction probability) would depend on the number of divisions, while in our model it depends on the population size. The dependence of mutations on the birth rate would change some of our results, especially the results on death rate and turnover.

When should two-strike therapy be used? Two-strike therapy holds most promise as an alternative to conventional sequential therapy – in which the second treatment is given only after the first has been seen to fail – especially in cases where a very good initial response to treatment is typically followed by relapse. We have shown it may be a wise choice when one of two available treatments is less effective than the other. Although our results suggest that two-strike therapy is likely to succeed only in relatively small tumours (Figure 5(A)), we expect that subsequent treatment strikes, following the same principle, would lead to higher extinction probabilities for larger tumours. Our predicted extinction probabilities for two-strike therapy are moreover conservative as we have assumed a much larger initial resistant population than expected for our default tumour size, according to a standard model of mutation-selection balance (see Appendix 1: Analytic Model Without Competition). Allee effects might

further increase extinction probabilities and make two-strike therapy viable in a wider range of scenarios (Dennis *et al.* 2016; Gatenby *et al.* 2020). Nevertheless, if resistant cells are abundant and have relatively high fitness then extinction may be practically unachievable and a long-term tumour control strategy such as adaptive therapy could be a better option (Gatenby *et al.* 2009; Monro and Gaffney 2009; Hansen and Read 2020; Viossat and Noble 2021).

When tolerable, combination therapy (that is, applying both treatments simultaneously) should also be considered. Whether it is better to apply drugs together or in sequence depends on several factors including the doses that can be administered in each case, the shape of the dose-response curves, the extent of synergism, and the degree of cross-resistance (Bozic *et al.* 2013; Dabi *et al.* 2025; Saputra *et al.* 2018; Nyhoegen *et al.* 2024). A comprehensive comparison of these alternative strategies using our mathematical methods is beyond the scope of the current study and remains an important topic for future research (but see Appendix 6: Comparison with combination therapy).

Even when it may be theoretically optimal, two-strike therapy crucially depends on the availability of effective treatments with low cross-resistance and methods for monitoring tumour burden over time (Reed *et al.* 2020). Moreover, even when it is predicted to be the best strategy, some patients and physicians might be reluctant to initiate a second treatment before the first has been seen to fail.

Demonstrating the breadth of potential applications of two-strike therapy, the three clinical trials that are already underway in metastatic rhabdomyosarcoma (NCT04388839 2020), metastatic prostate cancer (NCT05189457 2021), and metastatic breast cancer (NCT06409390 2024) involve not only diverse cancer types but also very different classes of treatment, including chemotherapy, targeted therapies, and hormonal agents. Other proposed targets include locally advanced rectal adenocarcinoma (Felder *et al.* 2021) and paediatric sarcomas (Reed *et al.* 2020).

Designing practical two-strike strategies. Given that the optimal switching size is reached some time after the tumour becomes undetectable, the design of practical switching strategies remains a challenging problem. One approach is to use a proxy for tumour size, such as prostate-specific antigen in the case of prostate cancer (NCT05189457 2021). But when personalized strategies are impractical it will be necessary to determine which standardized protocol performs best for a given cohort. Mathematical models and *in silico* trials have potential to facilitate this process by accounting for biological variation and clinical constraints as well as stochasticity (Dabi *et al.* 2025; Gallagher *et al.* 2025).

One idea is to extract tumour demographic rates by monitoring the decay in tumour volume during treatment (Grassberger *et al.* 2019), and to use sequencing data or experiments with patient-derived cells to estimate the initial size and growth rate of the resistant subpopulation. Using these parameter values, an estimator for when to switch could be constructed.

Conclusion and future directions. We have shown that two-strike therapy is a theoretically sound concept that, in certain scenarios, could plausibly increase cancer cure rates compared to conventional single-strike or sequential treatment strategies. Our work provides a necessary foundation for further mathematical investigation and justification for experimental and clinical testing of this innovative strategy.

An important topic for further mathematical analysis is the prevention of evolutionary rescue with more than two strikes. Previous work on the optimal scheduling of multiple treatments (Goldie *et al.* 1982; Coldman and Goldie 1983; Chen *et al.* 2013) suggests that alternating two treatments is a theoretically sound approach. An alternative strategy, more in line with the original conception of multi-strike therapy, is to switch to a third treatment whenever possible. Other, related directions for mathematical investigation include accounting for cross-resistance and considering alternative biological assumptions, such as modelling resistance as a continuous, plastic trait.

Data and code availability

The authors affirm that all data necessary for confirming the conclusions of the article are present within the article, figures, and tables. All relevant code is available in a public repository at https://doi.org/10.5281/zenodo.13332990.

Acknowledgements

We are grateful for the use of City St George's Hyperion cluster to run simulations integral to this study. We thank Jasmine Foo for helpful discussions about modelling combination therapy.

Funding

SP and RN were supported by the National Cancer Institute of the National Institutes of Health under Award Number U54CA217376. YN benefited from the European Union's Horizon 2020 research and innovation programme under the Marie Skłodowska-Curie grant agreement No 955708. YN and RN were also supported by a London Mathematical Society Research in Pairs award (reference 42320). The opinions expressed in this document reflect only the author's view and in no way reflect the European Commission's opinions. The European Commission is not responsible for any use that may be made of the information it contains. The content is solely the responsibility of the authors and does not necessarily represent the official views of the National Institutes of Health.

Competing Interests

We declare that we have no competing interests.

Contributions

RN conceived the research question. RN and YV supervised the project. SP and RN designed the research. SP developed the models. SP and AA ran simulations. SP, AA and YV carried out the mathematical analysis. SP wrote the paper with contributions from AA, YV and RN. All authors approved the manuscript.

Literature cited

Aktipis CA, Kwan VSY, Johnson KA, Neuberg SL, Maley CC. 2011. Overlooking Evolution: A Systematic Analysis of Cancer Relapse and Therapeutic Resistance Research. PLOS ONE. 6:e26100.

Alexander HK, Martin G, Martin OY, Bonhoeffer S. 2014. Evolutionary rescue: linking theory for conservation and medicine. Evolutionary Applications. 7:1161–1179.

Azimzade Y, Saberi AA, Gatenby RA. 2021. Superlinear growth reveals the allee effect in tumors. Phys. Rev. E. 103:042405.

Bell G. 2017. Evolutionary Rescue. Annual Review of Ecology, Evolution, and Systematics. 48:605–627.
Bozic I, Reiter JG, Allen B, Antal T, Chatterjee K, Shah P, Moon YS, Yaqubie A, Kelly N, Le DT *et al*. 2013. Evolutionary dynamics of cancer in response to targeted combination therapy. eLife. 2:e00747.
Chakrabarti S, Michor F. 2017. Pharmacokinetics and Drug Interactions Determine Optimum Combination Strategies in Computational Models of Cancer Evolution. Cancer Research. 77:3908–3921.
Chen JH, Kuo YH, Luh HP. 2013. Optimal policies of non-cross-resistant chemotherapy on Goldie and Coldman's cancer model. Mathematical Biosciences. 245:282–298.
Coldman A, Goldie J. 1983. A model for the resistance of tumor cells to cancer chemotherapeutic agents. Mathematical Biosciences. 65:291–307.
Dabi A, Brown JS, Gatenby RA, Jones CD, Schrider DR. 2025. Evolutionary rescue model informs strategies for driving cancer cell populations to extinction. bioRxiv. .
Day T, Read AF. 2016. Does high-dose antimicrobial chemotherapy prevent the evolution of resistance? PLOS Computational Biology. 12:1–20.
Dennis B, Assas L, Elaydi S, Kwessi E, Livadiotis G. 2016. Allee effects and resilience in stochastic populations. Theoretical Ecology. 9:323–335.
Enriquez-Navas PM, Wojtkowiak JW, Gatenby RA. 2015. Application of Evolutionary Principles to Cancer Therapy. Cancer Research. 75:4675–4680.
Felder SI, Fleming JB, Gatenby RA. 2021. Treatment-induced evolutionary dynamics in nonmetastatic locally advanced rectal adenocarcinoma, In: , Elsevier. volume 151. pp. 39–67.
Gallagher K, Strobl MA, Anderson AR, Maini PK. 2025. Deriving optimal treatment timing for adaptive therapy: Matching the model to the tumor dynamics. medRxiv. pp. 2025–04.
Gatenby RA, Artzy-Randrup Y, Epstein T, Reed DR, Brown JS. 2020. Eradicating metastatic cancer and the eco-evolutionary dynamics of Anthropocene extinctions. Cancer Research. 80:613–623.
Gatenby RA, Brown JS. 2020. Integrating evolutionary dynamics into cancer therapy. Nature Reviews Clinical Oncology. 17:675–686. Number: 11 Publisher: Nature Publishing Group.
Gatenby RA, Silva AS, Gillies RJ, Frieden BR. 2009. Adaptive therapy. Cancer Research. 69:4894–4903.
Gatenby RA, Zhang J, Brown JS. 2019. First strike-second strike strategies in metastatic cancer: Lessons from the evolutionary dynamics of extinction. Cancer Research. 79:3174–3177.
Gerlee P, Altrock PM, Malik A, Krona C, Nelander S. 2022. Autocrine signaling can explain the emergence of allee effects in cancer cell populations. PLOS Computational Biology. 18:1–15.
Getz W. 1975. Optimal control of a birth-and-death process population model. Mathematical Biosciences. 23:87–111.
Gillespie DT. 1977. Exact stochastic simulation of coupled chemical reactions. The Journal of Physical Chemistry. 81:2340–2361.
Goldie J, Coldman A, Gudauskas G. 1982. Rationale for the Use of Alternating Non -Cross - Resistant Chemotherapy. Cancer Treatment Reports. 66.
Gomulkiewicz R, Holt RD. 1995. When does evolution by natural selection prevent extinction? Evolution. pp. 201–207.
Grassberger C, McClatchy, David I, Geng C, Kamran SC, Fintelmann F, Maruvka YE, Piotrowska Z, Willers H, Sequist LV, Hata AN *et al*. 2019. Patient-specific tumor growth trajectories determine persistent and resistant cancer cell populations during treatment with targeted therapies. Cancer Research. 79:3776–3788.
Greaves M, Maley CC. 2012. Clonal evolution in cancer. Nature. 481:306–313. Number: 7381 Publisher: Nature Publishing Group.
Greenspoon PB, Mideo N. 2017. Evolutionary rescue of a parasite population by mutation rate evolution. Theoretical Population Biology. 117:64–75.
Hansen E, Read AF. 2020. Cancer therapy: Attempt cure or manage drug resistance? Evolutionary Applications. 13:1660–1672.
Iwasa Y, Michor F, Nowak MA. 2004. Evolutionary dynamics of invasion and escape. Journal of Theoretical Biology. 226:205–214.
Iwasa Y, Nowak MA, Michor F. 2006. Evolution of Resistance During Clonal Expansion. Genetics. 172:2557–2566.
Korolev KS, Xavier JB, Gore J. 2014. Turning ecology and evolution against cancer. Nature Reviews Cancer. 14:371–380.
Lambert A. 2006. Probability of fixation under weak selection: A branching process unifying approach. Theoretical Population Biology. 69:419–441.
Lamperti J. 1967. Continuous state branching processes. Bulletin of the American Mathematical Society. 73:382 – 386.
Marrec L, Bank C. 2023. Evolutionary rescue in a fluctuating environment: periodic versus quasi-periodic environmental changes. Proceedings of the Royal Society B: Biological Sciences. 290:20230770.
Marrec L, Bitbol AF. 2020. Resist or perish: Fate of a microbial population subjected to a periodic presence of antimicrobial. PLOS Computational Biology. 16:1–19.
Martin G, Aguilée R, Ramsayer J, Kaltz O, Ronce O. 2013. The probability of evolutionary rescue: towards a quantitative comparison between theory and evolution experiments. Philosophical Transactions of the Royal Society B: Biological Sciences. 368:20120088.
Monro HC, Gaffney EA. 2009. Modelling chemotherapy resistance in palliation and failed cure. Journal of Theoretical Biology. 257:292–302.
NCT04388839. 2020. Nct04388839: Evolutionary Inspired Therapy for Newly Diagnosed, Metastatic, Fusion Positive Rhabdomyosarcoma.
NCT05189457. 2021. Nct05189457: A Phase IIA Study of Sequential ("First Strike, Second Strike") Therapies, Modeled on Evolutionary Dynamics of Anthropocene Extinctions, for High Risk Metastatic Castration Sensitive Prostate Cancer.
NCT06409390. 2024. Nct06409390: A Pilot Study of Sequential ("First Strike, Second Strike") Therapies, Modeled on Evolutionary Dynamics of Anthropocene Extinctions, for Hormone Positive Metastatic Breast Cancer.
Nyhoegen C, Bonhoeffer S, Uecker H. 2024. The many dimensions of combination therapy: How to combine antibiotics to limit resistance evolution. Evolutionary Applications. 17:e13764. e13764 EVA-2023-262-OA.R1.
Orr HA, Unckless RL. 2008. Population Extinction and the Genetics of Adaptation. The American Naturalist. 172:160–169.
Orr HA, Unckless RL. 2014. The Population Genetics of Evolutionary Rescue. PLOS Genetics. 10:e1004551.
Osmond MM, Otto SP, Martin G. 2020. Genetic Paths to Evolutionary Rescue and the Distribution of Fitness Effects Along Them. Genetics. 214:493–510.
Otto SP, Whitlock MC. 1997. The Probability of Fixation in Popu-

lations of Changing Size. Genetics. 146:723–733.
Pressley M, Salvioli M, Lewis DB, Richards CL, Brown JS, Staňková K. 2021. Evolutionary Dynamics of Treatment-Induced Resistance in Cancer Informs Understanding of Rapid Evolution in Natural Systems. Frontiers in Ecology and Evolution. 9.
Raatz M, Traulsen A. 2023. Promoting extinction or minimizing growth? the impact of treatment on trait trajectories in evolving populations. Evolution. 77:1408–1421.
Reed DR, Metts J, Pressley M, Fridley BL, Hayashi M, Isakoff MS, Loeb DM, Makanji R, Roberts RD, Trucco M *et al*. 2020. An evolutionary framework for treating pediatric sarcomas. Cancer. 126:2577–2587. _eprint: https://onlinelibrary.wiley.com/doi/pdf/10.1002/cncr.32777.
Saputra EC, Huang L, Chen Y, Tucker-Kellogg L. 2018. Combination therapy and the evolution of resistance: The theoretical merits of synergism and antagonism in cancer. Cancer Research. 78:2419–2431.
Sewalt L, Harley K, van Heijster P, Balasuriya S. 2016. Influences of allee effects in the spreading of malignant tumours. Journal of Theoretical Biology. 394:77–92.
Strobl M, West J, Viossat Y, Damaghi M, Robertson-Tessi M, Brown J, Gatenby R, Maini P, Anderson A. 2020. Turnover modulates the need for a cost of resistance in adaptive therapy. Pages: 2020.01.22.914366 Section: New Results.
Torres-Barceló C, Arias-Sánchez FI, Vasse M, Ramsayer J, Kaltz O, Hochberg ME. 2014. A window of opportunity to control the bacterial pathogen pseudomonas aeruginosa combining antibiotics and phages. PloS one. 9:e106628.
Uecker H, Hermisson J. 2011. On the fixation process of a beneficial mutation in a variable environment. Genetics. 188:915–930.
Uecker H, Hermisson J. 2016. The role of recombination in evolutionary rescue. Genetics. 202:721–732.
Uecker H, Otto SP, Hermisson J. 2014. Evolutionary Rescue in Structured Populations. The American Naturalist. 183:E17–E35.
Viossat Y, Noble R. 2021. A theoretical analysis of tumour containment. Nature Ecology and Evolution. 5:826–835.
West J, Adler F, Gallaher J, Strobl M, Brady-Nicholls R, Brown J, Roberson-Tessi M, Kim E, Noble R, Viossat Y *et al*. 2023. A survey of open questions in adaptive therapy: Bridging mathematics and clinical translation. eLife. 12:e84263. Publisher: eLife Sciences Publications, Ltd.